The triangular lag window, also known as the Bartlett or Fejér window, given by

$$w(x) = 1 - |x|, \quad |x| \le 1$$

leads to the Fejér smoothing window:

$$W(\omega) = \frac{\sin^2(\pi r\omega)}{r\sin^2(\pi\omega)}.$$

In this case, (4.73) yields

$$\text{var}\{\widetilde{f}(\omega)\} \approx \frac{2r}{3n} f^2(\omega).$$

The idealized rectangular smoothing window, also called the Daniell window, is given by

$$W(\omega) = \begin{cases} r & |\omega| \le 1/2r, \\ 0 & \text{otherwise}, \end{cases}$$

and leads to the sinc lag window, namely

$$w(x) = \frac{\sin(\pi x)}{\pi x}, \quad |x| \le 1.$$

From (4.73) we have

$$\text{var}\{\widetilde{f}(\omega)\} \approx \frac{r}{n} f^2(\omega).$$

For lag window estimators, the width of the idealized rectangular window that leads to the same asymptotic variance as a given lag window estimator is sometimes called the equivalent bandwidth. For example, the bandwidth of the idealized rectangular window is $b_r = 1/r$ and the asymptotic variance is $\frac{1}{nb_r} f^2$. The asymptotic variance of the triangular window is $\frac{2r}{3n} f^2$, so setting $\frac{1}{nb_r} f^2 = \frac{2r}{3n} f^2$ and solving we get $b_r = 3/2r$ as the equivalent bandwidth.

4.6 Parametric Spectral Estimation

The methods of §4.5 lead to estimators generally referred to as nonparametric spectra because no assumption is made about the parametric form of the spectral density. In Property 4.3, we exhibited the spectrum of an ARMA process and we might consider basing a spectral estimator on this function, substituting the parameter estimates from an ARMA(p, q) fit on the data into the formula for the spectral density $f_x(\omega)$ given in (4.15). Such an estimator is called a parametric spectral estimator. For convenience, a parametric spectral estimator is obtained by fitting an AR(p) to the data, where the order p is determined by one of the model selection criteria, such as AIC, AICc, and BIC, defined in (2.19)-(2.21). Parametric autoregressive spectral estimators will often have superior resolution in problems when several closely spaced narrow

spectral peaks are present and are preferred by engineers for a broad variety of problems (see Kay, 1988). The development of autoregressive spectral estimators has been summarized by Parzen (1983).

If $\widehat{\phi}_1, \widehat{\phi}_2, \ldots, \widehat{\phi}_p$ and $\widehat{\sigma}_w^2$ are the estimates from an AR(p) fit to x_t, then based on Property 4.3, a parametric spectral estimate of $f_x(\omega)$ is attained by substituting these estimates into (4.15), that is,

$$\widehat{f}_x(\omega) = \frac{\widehat{\sigma}_w^2}{|\widehat{\phi}(\mathrm{e}^{-2\pi i\omega})|^2}, \tag{4.75}$$

where

$$\widehat{\phi}(z) = 1 - \widehat{\phi}_1 z - \widehat{\phi}_2 z^2 - \cdots - \widehat{\phi}_p z^p. \tag{4.76}$$

The asymptotic distribution of the autoregressive spectral estimator has been obtained by Berk (1974) under the conditions $p \to \infty$, $p^3/n \to 0$ as $p,\ n \to \infty$, which may be too severe for most applications. The limiting results imply a confidence interval of the form

$$\frac{\widehat{f}_x(\omega)}{(1 + Cz_{\alpha/2})} \le f_x(\omega) \le \frac{\widehat{f}_x(\omega)}{(1 - Cz_{\alpha/2})}, \tag{4.77}$$

where $C = \sqrt{2p/n}$ and $z_{\alpha/2}$ is the ordinate corresponding to the upper $\alpha/2$ probability of the standard normal distribution. If the sampling distribution is to be checked, we suggest applying the bootstrap estimator to get the sampling distribution of $\widehat{f}_x(\omega)$ using a procedure similar to the one used for $p = 1$ in Example 3.35. An alternative for higher order autoregressive series is to put the AR(p) in state-space form and use the bootstrap procedure discussed in §6.7.

An interesting fact about rational spectra of the form (4.15) is that any spectral density can be approximated, arbitrarily close, by the spectrum of an AR process.

Property 4.5 AR Spectral Approximation

Let $g(\omega)$ be the spectral density of a stationary process. Then, given $\epsilon > 0$, there is a time series with the representation

$$x_t = \sum_{k=1}^{p} \phi_k x_{t-k} + w_t$$

where w_t is white noise with variance σ_w^2, such that

$$|f_x(\omega) - g(\omega)| < \epsilon \quad \text{forall } \omega \in [-1/2, 1/2].$$

Moreover, p is finite and the roots of $\phi(z) = 1 - \sum_{k=1}^{p} \phi_k z^k$ are outside the unit circle.

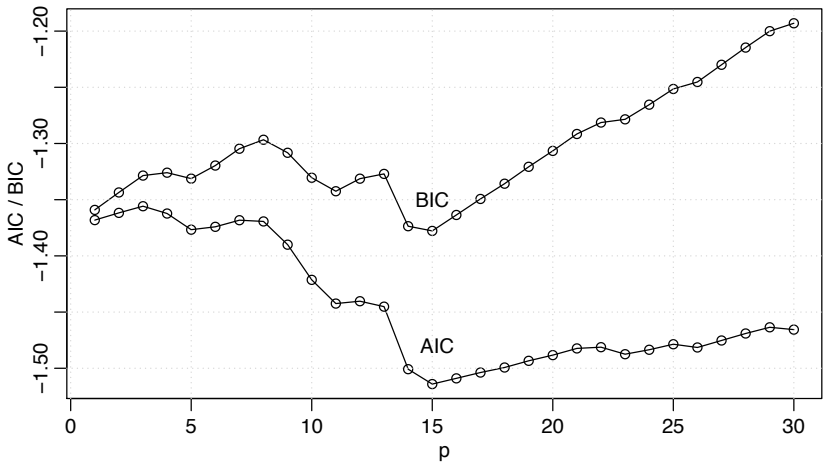

Fig. 4.11. Model selection criteria AIC and BIC as a function of order p for autoregressive models fitted to the SOI series.

One drawback of the property is that it does not tell us how large p must be before the approximation is reasonable; in some situations p may be extremely large. Property 4.5 also holds for MA and for ARMA processes in general, and a proof of the result may be found in Fuller (1996, Ch 4). We demonstrate the technique in the following example.

Example 4.15 Autoregressive Spectral Estimator for SOI

Consider obtaining results comparable to the nonparametric estimators shown in Figure 4.5 for the SOI series. Fitting successively higher order AR(p) models for $p = 1, 2, \ldots, 30$ yields a minimum BIC and a minimum AIC at $p = 15$, as shown in Figure 4.11. We can see from Figure 4.11 that BIC is very definite about which model it chooses; that is, the minimum BIC is very distinct. On the other hand, it is not clear what is going to happen with AIC; that is, the minimum is not so clear, and there is some concern that AIC will start decreasing after $p = 30$. Minimum AICc selects the $p = 15$ model, but suffers from the same uncertainty as AIC. The spectrum is shown in Figure 4.12, and we note the strong peaks at 52 months and 12 months corresponding to the nonparametric estimators obtained in §4.5. In addition, the harmonics of the yearly period are evident in the estimated spectrum.

To perform a similar analysis in R, the command `spec.ar` can be used to fit the best model via AIC and plot the resulting spectrum. A quick way to obtain the AIC values is to run the `ar` command as follows.

```
spaic = spec.ar(soi, log="no")     # min AIC spec
abline(v=frequency(soi)*1/52, lty="dotted")  # El Nino Cycle
(soi.ar = ar(soi, order.max=30))  # estimates and AICs
dev.new()
plot(1:30, soi.ar$aic[-1], type="o")   # plot AICs
```

R works only with the AIC in this case. To generate Figure 4.11 we used the following code to obtain AIC, AICc, and BIC. Because AIC and AICc

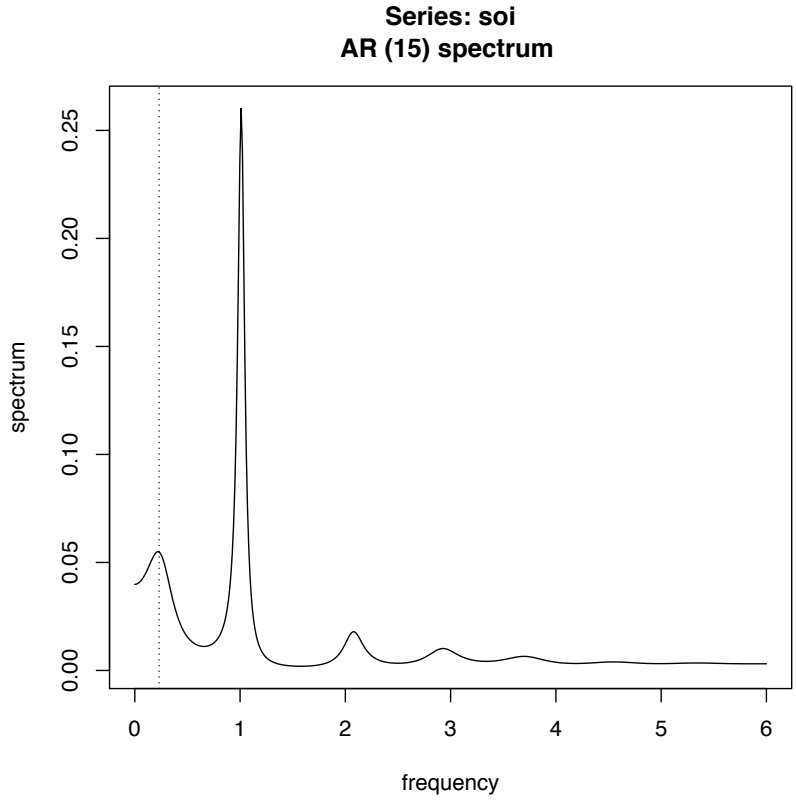

Fig. 4.12. Autoregressive spectral estimator for the SOI series using the AR(15) model selected by AIC, AICc, and BIC. The first peak (marked by a vertical dotted line) corresponds to the El Niño period of 52 months.

are nearly identical in this example, we only graphed AIC and BIC+1; we added 1 to the BIC to reduce white space in the graphic.

```
n = length(soi)
AIC = rep(0, 30) -> AICc -> BIC
for (k in 1:30){
 sigma2 = ar(soi, order=k, aic=FALSE)$var.pred
 BIC[k] = log(sigma2) + (k*log(n)/n)
 AICc[k] = log(sigma2) + ((n+k)/(n-k-2))
 AIC[k] = log(sigma2) + ((n+2*k)/n)
}
IC = cbind(AIC, BIC+1)
ts.plot(IC, type="o", xlab="p", ylab="AIC / BIC")
```

Finally, it should be mentioned that any parametric spectrum, say $f(\omega;\boldsymbol{\theta})$, depending on the vector parameter $\boldsymbol{\theta}$ can be estimated via the Whittle likelihood (Whittle, 1961), using the approximate properties of the discrete Fourier transform derived in Appendix C. We have that the DFTs, $d(\omega_j)$, are approximately complex normally distributed with mean zero and variance $f(\omega_j;\boldsymbol{\theta})$ and are approximately independent for $\omega_j \neq \omega_k$. This implies that an approximate log likelihood can be written in the form

$$\ln L(\boldsymbol{x};\boldsymbol{\theta}) \approx -\sum_{0<\omega_j<1/2}\left(\ln f_x(\omega_j;\boldsymbol{\theta}) + \frac{|d(\omega_j)|^2}{f_x(\omega_j;\boldsymbol{\theta})}\right), \tag{4.78}$$

where the sum is sometimes expanded to include the frequencies $\omega_j = 0, 1/2$. If the form with the two additional frequencies is used, the multiplier of the sum will be unity, except for the purely real points at $\omega_j = 0, 1/2$ for which the multiplier is $1/2$. For a discussion of applying the Whittle approximation to the problem of estimating parameters in an ARMA spectrum, see Anderson (1978). The Whittle likelihood is especially useful for fitting long memory models that will be discussed in Chapter 5.

4.7 Multiple Series and Cross-Spectra

The notion of analyzing frequency fluctuations using classical statistical ideas extends to the case in which there are several jointly stationary series, for example, x_t and y_t. In this case, we can introduce the idea of a correlation indexed by frequency, called the coherence. The results in Appendix C, §C.2, imply the covariance function

$$\gamma_{xy}(h) = E[(x_{t+h} - \mu_x)(y_t - \mu_y)]$$

has the representation

$$\gamma_{xy}(h) = \int_{-1/2}^{1/2} f_{xy}(\omega)\mathrm{e}^{2\pi i\omega h}\, d\omega \quad h = 0, \pm1, \pm2, ..., \tag{4.79}$$

where the cross-spectrum is defined as the Fourier transform

$$f_{xy}(\omega) = \sum_{h=-\infty}^{\infty} \gamma_{xy}(h)\ \mathrm{e}^{-2\pi i\omega h} \quad -1/2 \le \omega \le 1/2, \tag{4.80}$$

assuming that the cross-covariance function is absolutely summable, as was the case for the autocovariance. The cross-spectrum is generally a complex-valued function, and it is often written as[14]

$$f_{xy}(\omega) = c_{xy}(\omega) - iq_{xy}(\omega), \tag{4.81}$$

where

$$c_{xy}(\omega) = \sum_{h=-\infty}^{\infty} \gamma_{xy}(h)\ \cos(2\pi\omega h) \tag{4.82}$$

and

[14] For this section, it will be useful to recall the facts $e^{-i\alpha} = \cos(\alpha) - i\sin(\alpha)$ and if $z = a + ib$, then $\overline{z} = a - ib$.

$$q_{xy}(\omega) = \sum_{h=-\infty}^{\infty} \gamma_{xy}(h)\ \sin(2\pi\omega h) \tag{4.83}$$

are defined as the cospectrum and quadspectrum, respectively. Because of the relationship $\gamma_{yx}(h) = \gamma_{xy}(-h)$, it follows, by substituting into (4.80) and rearranging, that

$$f_{yx}(\omega) = \overline{f_{xy}(\omega)}. \tag{4.84}$$

This result, in turn, implies that the cospectrum and quadspectrum satisfy

$$c_{yx}(\omega) = c_{xy}(\omega) \tag{4.85}$$

and

$$q_{yx}(\omega) = -q_{xy}(\omega). \tag{4.86}$$

An important example of the application of the cross-spectrum is to the problem of predicting an output series y_t from some input series x_t through a linear filter relation such as the three-point moving average considered below. A measure of the strength of such a relation is the squared coherence function, defined as

$$\rho^2_{y\cdot x}(\omega) = \frac{|f_{yx}(\omega)|^2}{f_{xx}(\omega) f_{yy}(\omega)}, \tag{4.87}$$

where $f_{xx}(\omega)$ and $f_{yy}(\omega)$ are the individual spectra of the x_t and y_t series, respectively. Although we consider a more general form of this that applies to multiple inputs later, it is instructive to display the single input case as (4.87) to emphasize the analogy with conventional squared correlation, which takes the form

$$\rho^2_{yx} = \frac{\sigma^2_{yx}}{\sigma^2_x \sigma^2_y},$$

for random variables with variances σ^2_x and σ^2_y and covariance $\sigma_{yx} = \sigma_{xy}$. This motivates the interpretation of squared coherence and the squared correlation between two time series at frequency ω.

Example 4.16 Three-Point Moving Average

As a simple example, we compute the cross-spectrum between x_t and the three-point moving average $y_t = (x_{t-1}+x_t+x_{t+1})/3$, where x_t is a stationary input process with spectral density $f_{xx}(\omega)$. First,

$$\begin{aligned}
\gamma_{xy}(h) &= \operatorname{cov}(x_{t+h}, y_t) = \tfrac{1}{3}\operatorname{cov}(x_{t+h}, x_{t-1} + x_t + x_{t+1}) \\
&= \frac{1}{3}\big(\gamma_{xx}(h+1) + \gamma_{xx}(h) + \gamma_{xx}(h-1)\big) \\
&= \frac{1}{3}\int_{-1/2}^{1/2} \big(\mathrm{e}^{2\pi i\omega} + 1 + \mathrm{e}^{-2\pi i\omega}\big)\, \mathrm{e}^{2\pi i\omega h} f_{xx}(\omega)\, d\omega \\
&= \frac{1}{3}\int_{-1/2}^{1/2} [1 + 2\cos(2\pi\omega)] f_{xx}(\omega) \mathrm{e}^{2\pi i\omega h}\, d\omega,
\end{aligned}$$

where we have use (4.11). Using the uniqueness of the Fourier transform, we argue from the spectral representation (4.79) that

$$f_{xy}(\omega) = \tfrac{1}{3}\left[1 + 2\cos(2\pi\omega)\right] f_{xx}(\omega)$$

so that the cross-spectrum is real in this case. From Example 4.5, the spectral density of y_t is

$$\begin{aligned} f_{yy}(\omega) &= \tfrac{1}{9}[3 + 4\cos(2\pi\omega) + 2\cos(4\pi\omega)] f_{xx}(\omega) \\ &= \tfrac{1}{9}\left[1 + 2\cos(2\pi\omega)\right]^2 f_{xx}(\omega), \end{aligned}$$

using the identity $\cos(2\alpha) = 2\cos^2(\alpha) - 1$ in the last step. Substituting into (4.87) yields the squared coherence between x_t and y_t as unity over all frequencies. This is a characteristic inherited by more general linear filters, as will be shown in Problem 4.23. However, if some noise is added to the three-point moving average, the coherence is not unity; these kinds of models will be considered in detail later.

Property 4.6 Spectral Representation of a Vector Stationary Process

If the elements of the $p \times p$ autocovariance function matrix

$$\Gamma(h) = E[(\boldsymbol{x}_{t+h} - \boldsymbol{\mu})(\boldsymbol{x}_t - \boldsymbol{\mu})']$$

of a p-dimensional stationary time series, $\boldsymbol{x}_t = (x_{t1}, x_{t2}, \ldots, x_{tp})'$, has elements satisfying

$$\sum_{h=-\infty}^{\infty} |\gamma_{jk}(h)| < \infty \tag{4.88}$$

for all $j, k = 1, \ldots, p$, then $\Gamma(h)$ has the representation

$$\Gamma(h) = \int_{-1/2}^{1/2} \mathrm{e}^{2\pi i\omega h} f(\omega)\, d\omega \quad h = 0, \pm 1, \pm 2, \ldots, \tag{4.89}$$

as the inverse transform of the spectral density matrix, $f(\omega) = \{f_{jk}(\omega)\}$, for $j, k = 1, \ldots, p$, with elements equal to the cross-spectral components. The matrix $f(\omega)$ has the representation

$$f(\omega) = \sum_{h=-\infty}^{\infty} \Gamma(h)\mathrm{e}^{-2\pi i\omega h} \quad -1/2 \le \omega \le 1/2. \tag{4.90}$$

Example 4.17 Spectral Matrix of a Bivariate Process

Consider a jointly stationary bivariate process (x_t, y_t). We arrange the autocovariances in the matrix

$$\Gamma(h) = \begin{pmatrix} \gamma_{xx}(h) & \gamma_{xy}(h) \\ \gamma_{yx}(h) & \gamma_{yy}(h) \end{pmatrix}.$$

The spectral matrix would be given by

$$f(\omega) = \begin{pmatrix} f_{xx}(\omega) & f_{xy}(\omega) \\ f_{yx}(\omega) & f_{yy}(\omega) \end{pmatrix},$$

where the Fourier transform (4.89) and (4.90) relate the autocovariance and spectral matrices.

The extension of spectral estimation to vector series is fairly obvious. For the vector series $\boldsymbol{x}_t = (x_{t1}, x_{t2}, \ldots, x_{tp})'$, we may use the vector of DFTs, say $\boldsymbol{d}(\omega_j) = (d_1(\omega_j), d_2(\omega_j), \ldots, d_p(\omega_j))'$, and estimate the spectral matrix by

$$\bar{f}(\omega) = L^{-1} \sum_{k=-m}^{m} I(\omega_j + k/n) \tag{4.91}$$

where now

$$I(\omega_j) = \boldsymbol{d}(\omega_j)\, \boldsymbol{d}^*(\omega_j) \tag{4.92}$$

is a $p \times p$ complex matrix.[15]

Again, the series may be tapered before the DFT is taken in (4.91) and we can use weighted estimation,

$$\widehat{f}(\omega) = \sum_{k=-m}^{m} h_k\, I(\omega_j + k/n) \tag{4.93}$$

where $\{h_k\}$ are weights as defined in (4.56). The estimate of squared coherence between two series, y_t and x_t is

$$\widehat{\rho}^2_{y\cdot x}(\omega) = \frac{|\widehat{f}_{yx}(\omega)|^2}{\widehat{f}_{xx}(\omega)\widehat{f}_{yy}(\omega)}. \tag{4.94}$$

If the spectral estimates in (4.94) are obtained using equal weights, we will write $\bar{\rho}^2_{y\cdot x}(\omega)$ for the estimate.

Under general conditions, if $\rho^2_{y\cdot x}(\omega) > 0$ then

$$|\widehat{\rho}_{y\cdot x}(\omega)| \sim AN\left(|\rho_{y\cdot x}(\omega)|, \left(1 - \rho^2_{y\cdot x}(\omega)\right)^2 / 2L_h\right) \tag{4.95}$$

where L_h is defined in (4.57); the details of this result may be found in Brockwell and Davis (1991, Ch 11). We may use (4.95) to obtain approximate confidence intervals for the squared coherency $\rho^2_{y\cdot x}(\omega)$.

We can test the hypothesis that $\rho^2_{y\cdot x}(\omega) = 0$ if we use $\bar{\rho}^2_{y\cdot x}(\omega)$ for the estimate with $L > 1$,[16] that is,

[15] If Z is a complex matrix, then $Z^* = \overline{Z}'$ denotes the conjugate transpose operation. That is, Z^* is the result of replacing each element of Z by its complex conjugate and transposing the resulting matrix.

[16] If $L = 1$ then $\bar{\rho}^2_{y\cdot x}(\omega) \equiv 1$.

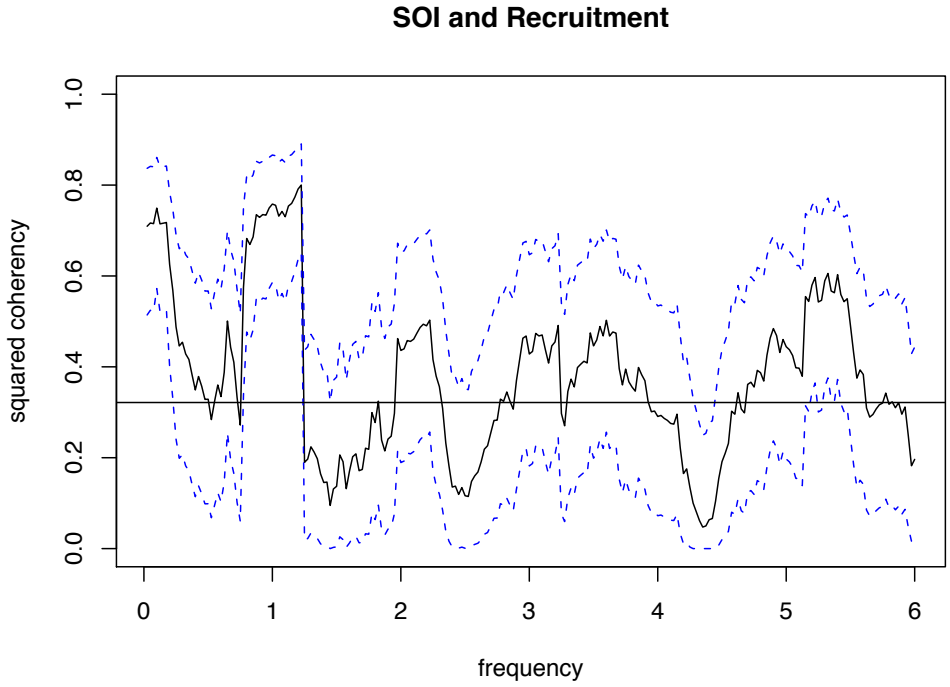

Fig. 4.13. Squared coherency between the SOI and Recruitment series; $L = 19$, $n = 453$, $n' = 480$, and $\alpha = .001$. The horizontal line is $C_{.001}$.

$$\bar{\rho}^2_{y\cdot x}(\omega) = \frac{|\bar{f}_{yx}(\omega)|^2}{\bar{f}_{xx}(\omega)\bar{f}_{yy}(\omega)}. \tag{4.96}$$

In this case, under the null hypothesis, the statistic

$$F = \frac{\bar{\rho}^2_{y\cdot x}(\omega)}{(1-\bar{\rho}^2_{y\cdot x}(\omega))}(L-1) \tag{4.97}$$

has an approximate F-distribution with 2 and $2L-2$ degrees of freedom. When the series have been extended to length n', we replace $2L-2$ by $df-2$, where df is defined in (4.52). Solving (4.97) for a particular significance level α leads to

$$C_\alpha = \frac{F_{2,2L-2}(\alpha)}{L-1+F_{2,2L-2}(\alpha)} \tag{4.98}$$

as the approximate value that must be exceeded for the original squared coherence to be able to reject $\rho^2_{y\cdot x}(\omega) = 0$ at an a priori specified frequency.

Example 4.18 Coherence Between SOI and Recruitment

Figure 4.13 shows the squared coherence between the SOI and Recruitment series over a wider band than was used for the spectrum. In this case, we used $L = 19$, $df = 2(19)(453/480) \approx 36$ and $F_{2,df-2}(.001) \approx 8.53$ at the significance level $\alpha = .001$. Hence, we may reject the hypothesis of no coherence for values of $\bar{\rho}^2_{y\cdot x}(\omega)$ that exceed $C_{.001} = .32$. We emphasize that this method

is crude because, in addition to the fact that the F-statistic is approximate, we are examining the squared coherence across all frequencies with the Bonferroni inequality, (4.55), in mind. Figure 4.13 also exhibits confidence bands as part of the R plotting routine. We emphasize that these bands are only valid for ω where $\rho^2_{y\cdot x}(\omega) > 0$.

In this case, the seasonal frequency and the El Niño frequencies ranging between about 3 and 7 year periods are strongly coherent. Other frequencies are also strongly coherent, although the strong coherence is less impressive because the underlying power spectrum at these higher frequencies is fairly small. Finally, we note that the coherence is persistent at the seasonal harmonic frequencies.

This example may be reproduced using the following R commands.

```
sr=spec.pgram(cbind(soi,rec),kernel("daniell",9),taper=0,plot=FALSE)
sr$df                    # df = 35.8625
f = qf(.999, 2, sr$df-2)  # = 8.529792
C = f/(18+f)              # = 0.318878
plot(sr, plot.type = "coh", ci.lty = 2)
abline(h = C)
```

4.8 Linear Filters

Some of the examples of the previous sections have hinted at the possibility the distribution of power or variance in a time series can be modified by making a linear transformation. In this section, we explore that notion further by defining a linear filter and showing how it can be used to extract signals from a time series. The linear filter modifies the spectral characteristics of a time series in a predictable way, and the systematic development of methods for taking advantage of the special properties of linear filters is an important topic in time series analysis.

A linear filter uses a set of specified coefficients a_j, for $j = 0, \pm1, \pm2, \ldots$, to transform an input series, x_t, producing an output series, y_t, of the form

$$y_t = \sum_{j=-\infty}^{\infty} a_j x_{t-j}, \qquad \sum_{j=-\infty}^{\infty} |a_j| < \infty. \tag{4.99}$$

The form (4.99) is also called a convolution in some statistical contexts. The coefficients, collectively called the *impulse response function*, are required to satisfy absolute summability so y_t in (4.99) exists as a limit in mean square and the infinite Fourier transform

$$A_{yx}(\omega) = \sum_{j=-\infty}^{\infty} a_j \, \mathrm{e}^{-2\pi i \omega j}, \tag{4.100}$$

called the *frequency response function*, is well defined. We have already encountered several linear filters, for example, the simple three-point moving

average in Example 4.16, which can be put into the form of (4.99) by letting $a_{-1} = a_0 = a_1 = 1/3$ and taking $a_t = 0$ for $|j| \geq 2$.

The importance of the linear filter stems from its ability to enhance certain parts of the spectrum of the input series. To see this, assuming that x_t is stationary with spectral density $f_{xx}(\omega)$, the autocovariance function of the filtered output y_t in (4.99) can be derived as

$$\begin{aligned}
\gamma_{yy}(h) &= \operatorname{cov}(y_{t+h}, y_t) \\
&= \operatorname{cov}\left(\sum_r a_r x_{t+h-r}, \sum_s a_s x_{t-s}\right) \\
&= \sum_r \sum_s a_r \gamma_{xx}(h-r+s) a_s \\
&= \sum_r \sum_s a_r \left[\int_{-1/2}^{1/2} \mathrm{e}^{2\pi i\omega(h-r+s)} f_{xx}(\omega) d\omega\right] a_s \\
&= \int_{-1/2}^{1/2} \left(\sum_r a_r \mathrm{e}^{-2\pi i\omega r}\right)\left(\sum_s a_s \mathrm{e}^{2\pi i\omega s}\right) \mathrm{e}^{2\pi i\omega h} f_{xx}(\omega)\ d\omega \\
&= \int_{-1/2}^{1/2} \mathrm{e}^{2\pi i\omega h} |A_{yx}(\omega)|^2 f_{xx}(\omega)\ d\omega,
\end{aligned}$$

where we have first replaced $\gamma_{xx}(\cdot)$ by its representation (4.11) and then substituted $A_{yx}(\omega)$ from (4.100). The computation is one we do repeatedly, exploiting the uniqueness of the Fourier transform. Now, because the left-hand side is the Fourier transform of the spectral density of the output, say, $f_{yy}(\omega)$, we get the important filtering property as follows.

Property 4.7 Output Spectrum of a Filtered Stationary Series

The spectrum of the filtered output y_t in (4.99) is related to the spectrum of the input x_t by

$$f_{yy}(\omega) = |A_{yx}(\omega)|^2\ f_{xx}(\omega), \tag{4.101}$$

where the frequency response function $A_{yx}(\omega)$ is defined in (4.100).

The result (4.101) enables us to calculate the exact effect on the spectrum of any given filtering operation. This important property shows the spectrum of the input series is changed by filtering and the effect of the change can be characterized as a frequency-by-frequency multiplication by the squared magnitude of the frequency response function. Again, an obvious analogy to a property of the variance in classical statistics holds, namely, if x is a random variable with variance σ_x^2, then $y = ax$ will have variance $\sigma_y^2 = a^2\sigma_x^2$, so the variance of the linearly transformed random variable is changed by multiplication by a^2 in much the same way as the linearly filtered spectrum is changed in (4.101).

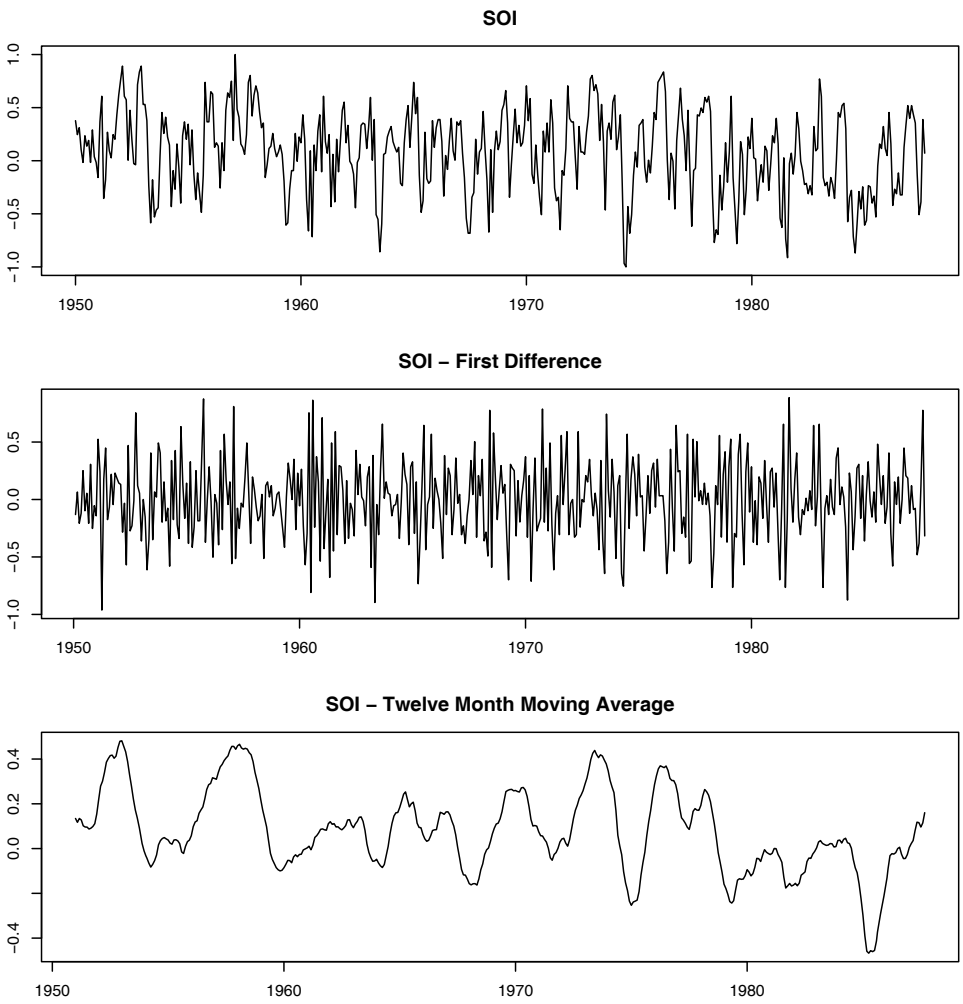

Fig. 4.14. SOI series (top) compared with the differenced SOI (middle) and a centered 12-month moving average (bottom).

Finally, we mention that Property 4.3, which was used to get the spectrum of an ARMA process, is just a special case of Property 4.7 where in (4.99), $x_t = w_t$ is white noise, in which case $f_{xx}(\omega) = \sigma_w^2$, and $a_j = \psi_j$, in which case

$$A_{yx}(\omega) = \psi(\mathrm{e}^{-2\pi i\omega}) = \theta(\mathrm{e}^{-2\pi i\omega}) \,/\, \phi(\mathrm{e}^{-2\pi i\omega}).$$

Example 4.19 First Difference and Moving Average Filters

We illustrate the effect of filtering with two common examples, the first difference filter

$$y_t = \nabla x_t = x_t - x_{t-1}$$

and the symmetric moving average filter

$$y_t = \tfrac{1}{24}\big(x_{t-6} + x_{t+6}\big) + \tfrac{1}{12}\sum_{r=-5}^{5} x_{t-r},$$

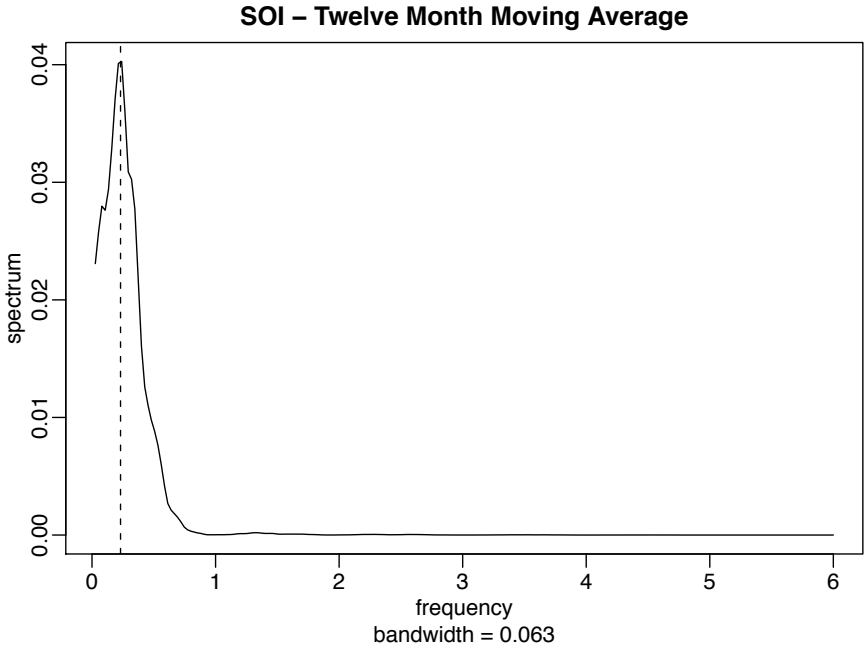

Fig. 4.15. Spectral analysis of SOI after applying a 12-month moving average filter. The vertical line corresponds to the 52-month cycle.

which is a modified Daniell kernel with $m = 6$. The results of filtering the SOI series using the two filters are shown in the middle and bottom panels of Figure 4.14. Notice that the effect of differencing is to roughen the series because it tends to retain the higher or faster frequencies. The centered moving average smoothes the series because it retains the lower frequencies and tends to attenuate the higher frequencies. In general, differencing is an example of a *high-pass filter* because it retains or passes the higher frequencies, whereas the moving average is a *low-pass filter* because it passes the lower or slower frequencies.

Notice that the slower periods are enhanced in the symmetric moving average and the seasonal or yearly frequencies are attenuated. The filtered series makes about 9 cycles in the length of the data (about one cycle every 52 months) and the moving average filter tends to enhance or extract the signal that is associated with El Niño. Moreover, by the low-pass filtering of the data, we get a better sense of the El Niño effect and its irregularity. Figure 4.15 shows the results of a spectral analysis on the low-pass filtered SOI series. It is clear that all high frequency behavior has been removed and the El Niño cycle is accentuated; the dotted vertical line in the figure corresponds to the 52 months cycle.

Now, having done the filtering, it is essential to determine the exact way in which the filters change the input spectrum. We shall use (4.100) and (4.101) for this purpose. The first difference filter can be written in the form (4.99) by letting $a_0 = 1, a_1 = -1$, and $a_r = 0$ otherwise. This implies that

$$A_{yx}(\omega) = 1 - \mathrm{e}^{-2\pi i\omega},$$

and the squared frequency response becomes

$$|A_{yx}(\omega)|^2 = (1 - \mathrm{e}^{-2\pi i\omega})(1 - \mathrm{e}^{2\pi i\omega}) = 2[1 - \cos(2\pi\omega)]. \tag{4.102}$$

The top panel of Figure 4.16 shows that the first difference filter will attenuate the lower frequencies and enhance the higher frequencies because the multiplier of the spectrum, $|A_{yx}(\omega)|^2$, is large for the higher frequencies and small for the lower frequencies. Generally, the slow rise of this kind of filter does not particularly recommend it as a procedure for retaining only the high frequencies.

For the centered 12-month moving average, we can take $a_{-6} = a_6 = 1/24$, $a_k = 1/12$ for $-5 \le k \le 5$ and $a_k = 0$ elsewhere. Substituting and recognizing the cosine terms gives

$$A_{yx}(\omega) = \tfrac{1}{12}\Big[1 + \cos(12\pi\omega) + 2\sum_{k=1}^{5}\cos(2\pi\omega k)\Big]. \tag{4.103}$$

Plotting the squared frequency response of this function as in Figure 4.16 shows that we can expect this filter to cut most of the frequency content above .05 cycles per point. This corresponds to eliminating periods shorter than $T = 1/.05 = 20$ points. In particular, this drives down the yearly components with periods of $T = 12$ months and enhances the El Niño frequency, which is somewhat lower. The filter is not completely efficient at attenuating high frequencies; some power contributions are left at higher frequencies, as shown in the function $|A_{yx}(\omega)|^2$ and in the spectrum of the moving average shown in Figure 4.3.

The following R session shows how to filter the data, perform the spectral analysis of this example, and plot the squared frequency response curve of the difference filter.

```
par(mfrow=c(3,1))
plot(soi)  # plot data
plot(diff(soi))  # plot first difference
k = kernel("modified.daniell", 6)  # filter weights
plot(soif <- kernapply(soi, k))    # plot 12 month filter
dev.new()
spectrum(soif, spans=9, log="no")  # spectral analysis
abline(v=12/52, lty="dashed")
dev.new()
w = seq(0, .5, length=500)  # frequency response
FR = abs(1-exp(2i*pi*w))^2
plot(w, FR, type="l")
```

The two filters discussed in the previous example were different in that the frequency response function of the first difference was complex-valued, whereas the frequency response of the moving average was purely real. A

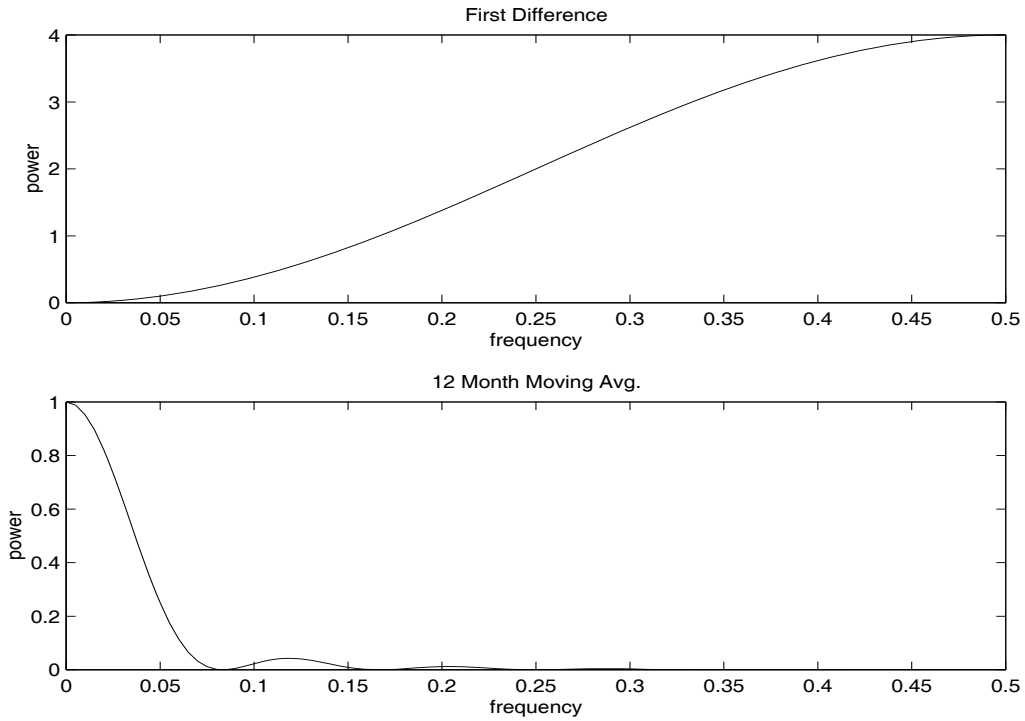

Fig. 4.16. Squared frequency response functions of the first difference and 12-month moving average filters.

short derivation similar to that used to verify (4.101) shows, when x_t and y_t are related by the linear filter relation (4.99), the cross-spectrum satisfies

$$f_{yx}(\omega) = A_{yx}(\omega) f_{xx}(\omega),$$

so the frequency response is of the form

$$A_{yx}(\omega) = \frac{f_{yx}(\omega)}{f_{xx}(\omega)} \tag{4.104}$$

$$= \frac{c_{yx}(\omega)}{f_{xx}(\omega)} - i\frac{q_{yx}(\omega)}{f_{xx}(\omega)}, \tag{4.105}$$

where we have used (4.81) to get the last form. Then, we may write (4.105) in polar coordinates as

$$A_{yx}(\omega) = |A_{yx}(\omega)| \ \exp\{-i \ \phi_{yx}(\omega)\}, \tag{4.106}$$

where the amplitude and phase of the filter are defined by

$$|A_{yx}(\omega)| = \frac{\sqrt{c_{yx}^2(\omega) + q_{yx}^2(\omega)}}{f_{xx}(\omega)} \tag{4.107}$$

and

$$\phi_{yx}(\omega) = \tan^{-1}\left(-\frac{q_{yx}(\omega)}{c_{yx}(\omega)}\right). \tag{4.108}$$

A simple interpretation of the phase of a linear filter is that it exhibits time delays as a function of frequency in the same way as the spectrum represents the variance as a function of frequency. Additional insight can be gained by considering the simple delaying filter

$$y_t = Ax_{t-D},$$

where the series gets replaced by a version, amplified by multiplying by A and delayed by D points. For this case,

$$f_{yx}(\omega) = A\mathrm{e}^{-2\pi i\omega D} f_{xx}(\omega),$$

and the amplitude is $|A|$, and the phase is

$$\phi_{yx}(\omega) = -2\pi\omega D,$$

or just a linear function of frequency ω. For this case, applying a simple time delay causes phase delays that depend on the frequency of the periodic component being delayed. Interpretation is further enhanced by setting

$$x_t = \cos(2\pi\omega t),$$

in which case

$$y_t = A\cos(2\pi\omega t - 2\pi\omega D).$$

Thus, the output series, y_t, has the same period as the input series, x_t, but the amplitude of the output has increased by a factor of $|A|$ and the phase has been changed by a factor of $-2\pi\omega D$.

Example 4.20 Difference and Moving Average Filters

We consider calculating the amplitude and phase of the two filters discussed in Example 4.19. The case for the moving average is easy because $A_{yx}(\omega)$ given in (4.103) is purely real. So, the amplitude is just $|A_{yx}(\omega)|$ and the phase is $\phi_{yx}(\omega) = 0$. In general, symmetric ($a_j = a_{-j}$) filters have zero phase. The first difference, however, changes this, as we might expect from the example above involving the time delay filter. In this case, the squared amplitude is given in (4.102). To compute the phase, we write

$$\begin{aligned} A_{yx}(\omega) &= 1 - e^{-2\pi i\omega} = e^{-i\pi\omega}(e^{i\pi\omega} - e^{-i\pi\omega}) \\ &= 2ie^{-i\pi\omega}\sin(\pi\omega) = 2\sin^2(\pi\omega) + 2i\cos(\pi\omega)\sin(\pi\omega) \\ &= \frac{c_{yx}(\omega)}{f_{xx}(\omega)} - i\frac{q_{yx}(\omega)}{f_{xx}(\omega)}, \end{aligned}$$

so

$$\phi_{yx}(\omega) = \tan^{-1}\left(-\frac{q_{yx}(\omega)}{c_{yx}(\omega)}\right) = \tan^{-1}\left(\frac{\cos(\pi\omega)}{\sin(\pi\omega)}\right).$$